

UCLA

UCLA Previously Published Works

Title

Trophic status of *Chlamydomonas reinhardtii* influences the impact of iron deficiency on photosynthesis

Permalink

<https://escholarship.org/uc/item/6fz1s983>

Journal

Photosynthesis Research: Official Journal of the International Society of Photosynthesis Research, 105(1)

ISSN

1573-5079

Authors

Terauchi, Aimee M.
Peers, Graham
Kobayashi, Marilyn C.
et al.

Publication Date

2010-07-01

DOI

10.1007/s11120-010-9562-8

Peer reviewed

Trophic status of *Chlamydomonas reinhardtii* influences the impact of iron deficiency on photosynthesis

Aimee M. Terauchi · Graham Peers ·
Marilyn C. Kobayashi · Krishna K. Niyogi ·
Sabeeha S. Merchant

Received: 12 February 2010 / Accepted: 12 May 2010 / Published online: 10 June 2010
© The Author(s) 2010. This article is published with open access at Springerlink.com

Abstract To investigate the impact of iron deficiency on bioenergetic pathways in *Chlamydomonas*, we compared growth rates, iron content, and photosynthetic parameters systematically in acetate versus CO₂-grown cells. Acetate-grown cells have, predictably (2-fold) greater abundance of respiration components but also, counter-intuitively, more chlorophyll on a per cell basis. We found that phototrophic cells are less impacted by iron deficiency and this correlates with their higher iron content on a per cell basis, suggesting a greater capacity/ability for iron assimilation in this metabolic state. Phototrophic cells maintain both photosynthetic and respiratory function and their associated Fe-containing proteins in conditions where heterotrophic cells lose photosynthetic capacity and have reduced oxygen evolution activity. Maintenance of NPQ capacity might contribute to protection of the photosynthetic apparatus in iron-limited phototrophic cells. Acetate-grown

iron-limited cells maintain high growth rates by suppressing photosynthesis but increasing instead respiration. These cells are also able to maintain a reduced plastoquinone pool.

Keywords Acetate · Algae · LhcSR · Non-photochemical quenching · Respiration

Abbreviations

PSI, PSII	Photosystem I, photosystem II
LHCI	Light harvesting complex I
NPQ	Non-photochemical quenching
HPLC	High performance liquid chromatography
SDS PAGE	Sodium dodecyl sulfate polyacrylamide gel electrophoresis

Electronic supplementary material The online version of this article (doi:10.1007/s11120-010-9562-8) contains supplementary material, which is available to authorized users.

A. M. Terauchi · S. S. Merchant (✉)
Department of Chemistry and Biochemistry, University
of California, Los Angeles, CA 90095-1569, USA
e-mail: sabeeha@chem.ucla.edu; merchant@chem.ucla.edu

G. Peers · M. C. Kobayashi · K. K. Niyogi
Department of Plant and Microbial Biology, University
of California, Berkeley, CA 94720-3102, USA

K. K. Niyogi
Physical Biosciences Division, Lawrence Berkeley National
Laboratory, Berkeley, CA 94720, USA

S. S. Merchant
Institute for Genomics and Proteomics, University of California,
Los Angeles, CA 90095, USA

Introduction

Although iron (Fe) is the fourth most abundant element in the Earth's crust, its low bioavailability makes it a limiting nutrient for life. In nature, iron is mostly found as stable Fe³⁺-oxides, which are insoluble in aerobic environments at biological pH (Guerinot and Yi 1994). Iron's control on photosynthetic systems has been notably demonstrated by the stimulation of algal blooms following the addition of nanomolar concentrations of iron to several open ocean locations that receive very low natural iron inputs (e.g., Martin et al. 1994; Boyd et al. 2000). Besides oceanic plankton communities, iron-deficiency has been well documented in plants and in heterotrophs. Organisms have developed complex systems for iron acquisition and for adjusting their biochemistries to survive in low iron

environments (reviewed in Guerinot 1994; Marschner and Römheld 1994; Philpott 2006; Walker and Connolly 2008).

The majority of iron in algae and plants is believed to be associated with the chloroplast (Raven 1988; Briat et al. 2007). In oxygenic photosynthesis, iron is a cofactor in PSII, PSI, the cytochrome *b₆/f* complex, and in algae, cytochrome *c₆* as well. The abundance of these proteins is reduced during iron-deficient growth (Singh et al. 2003). PSI seems to be a focus during iron limitation, probably due to its high iron content (12 Fe per PSI) (Sandmann and Malkin 1983). The ratio of PSI/PSII changes from 4:1 to 1:1 under iron deficiency in cyanobacteria (Straus 1995), and a diatom evolved to low ambient iron has a constitutive PSII/PSI ratio of about 10:1 (Strzepek and Harrison 2004).

A reduction in the number of reaction centers decreases the ability of the photosynthetic apparatus to use light energy, and iron-limited algae and cyanobacteria show decreased PSII function, inter-photosystem electron transport, carbon fixation rates, and ultimately decreased growth (Greene et al. 1992; Vassiliev et al. 1995; Ivanov et al. 2000). To compensate for the change in the abundance of photosystems, cyanobacteria modify their remaining photosystem I to maximize light harvesting while minimizing photooxidative damage (reviewed in Michel and Pistorius 2004; Kouril et al. 2005). In addition to these changes, some iron-containing electron carriers are replaced completely by iron-independent substitutes such as the well-characterized switch from ferredoxin to flavodoxin (Laudenbach et al. 1988; Sandmann et al. 1990; La Roche et al. 1995, 1996; Erdner et al. 1999). This phenomenon is known as metal sparing.

After the photosynthetic apparatus, the respiratory electron transport chain represents the major use of iron within a photosynthetic cell. Iron limitation should also impact its activity, and indeed, studies in land plants indicate that iron limitation causes a decrease in iron-containing respiratory complexes, oxygen consumption, and growth rate (Pascal and Douce 1993; López-Millán et al. 2000; Andaluz et al. 2006; Vigani et al. 2009). Iron limitation in heterotrophic bacteria also significantly impacts electron flow, oxygen consumption, and growth rates (Rainnie and Bragg 1973; Hubbard et al. 1986; Tortell et al. 1996).

Chlamydomonas reinhardtii, in the green plant lineage, is a reference organism for the study of chloroplast metabolism and photosynthesis. This unicellular alga can grow phototrophically in the light, heterotrophically with acetate in the dark, or mixotrophically on acetate in the light. In an experimental situation, four stages of iron nutrition can be distinguished (La Fontaine et al. 2002; Moseley et al. 2002; Long et al. 2008). Iron-replete, with 20- μM Fe in the medium, corresponds to the iron content of standard laboratory growth medium (Harris 2009). In the iron-deficiency state (1–3- μM Fe, depending on the strain)

the cells are preparing for the onset of iron limitation by up-regulating iron transporters and adjusting their biochemistry to minimize iron utilization, but their chlorophyll content is not or only marginally affected. Fluorescence kinetics and low temperature fluorescence studies indicate an impact on PSI light harvesting as well as electron transfer (Moseley et al. 2002). Iron-limited cultures (0.2- μM Fe) are visibly chlorotic owing to the programmed destruction of reaction centers and LHClS (Moseley et al. 2002; Naumann et al. 2005). The involvement of a di-iron aerobic cyclase encoded by *CHL27* in chlorophyll biosynthesis may also contribute to chlorosis (Tottey et al. 2003). Finally, in the iron-excess situation (200- μM Fe), the cells are phenotypically indistinguishable from iron-replete cells at normal light intensities but are sensitive to excess excitation energy (>500 $\mu\text{mol photons m}^{-2} \text{ s}^{-1}$) (Long and Merchant 2008).

We investigated the iron nutrition response of *Chlamydomonas* in acetate versus minimal medium to distinguish the impact of deficiency on bioenergetic pathways. There were striking differences in the response of the photosynthetic apparatus depending on the trophic status of the cultures. Iron-limited, photoheterotrophically grown cells maintained high growth rates by apparently suppressing photosynthesis while maintaining relatively high rates of respiration. This contrasts with autotrophic cells, which had efficient photosynthetic systems throughout the spectrum of iron nutritional status, but lost overall photosynthetic capacity at the onset of iron limitation.

Materials and methods

Strains and growth

Chlamydomonas reinhardtii strain 4A⁺ (137c background, courtesy of J.-D. Rochaix, University of Geneva) was used in this study. Starter cultures were maintained either photoheterotrophically in standard Tris–acetate–phosphate (TAP) medium or in autotrophic medium lacking acetate (TP) at 24°C at a light intensity of 95 $\mu\text{mol photons m}^{-2} \text{ s}^{-1}$ and constant shaking (Harris 2009). For TP medium, acetic acid was omitted from the medium and the pH was adjusted to 7.4 with HCl. Autotrophic cells were also bubbled with sterile air. Media containing various amounts of iron were prepared and inoculated as in (Terauchi et al. 2009). No significant differences in chemical speciation at equilibrium in TP vs. TAP or in TP versus HSM (which is commonly used in other studies) were predicted using Visual Minteq software (<http://www.lwr.kth.se/English/OurSoftware/vminteq>). Cells were collected in mid-exponential phase ($1\text{--}2 \times 10^6$ cells per ml) for all analyses.

Measurement of iron content

Samples were prepared as described by Petroustos et al. (2009) and iron content was determined by inductively coupled plasma-mass spectroscopy (Agilent 7500 ICP-MS, detection limit 0.01 ppb) using the standard addition method in Helium mode.

Protein isolation for immunoblot analysis

2×10^8 cells were collected by centrifugation at $2500 \times g$ for 3 min, washed in 10-mM sodium phosphate, pH 7.0, resuspended in 300 μ l of the same buffer, and stored at -80°C . For denaturing gel electrophoresis, cells were lysed by freeze/thaw cycling (Howe and Merchant 1992), and protein concentration was determined by the Lowry method against a Bovine Serum Albumin standard.

Immunodetection

Proteins were separated by SDS-PAGE and immunodetection was carried out essentially as by Terauchi et al. (2009) except that membrane protein samples were incubated at 65°C for 20 min prior to separation by SDS-PAGE and transferred to a polyvinylidene difluoride membrane in transfer buffer containing 0.04% SDS. Primary antibody dilutions were: Fd, 1:10 000; Cyt *f*, 1:1000; D1, 1:500; PsaD, 1:1000; LhcSR, 1:1000; Fox1, 1:300; Nuo6, 1:2000; Nuo7, 1:2000; Nuo8, 1:3000, Cox2b, 1:5000, CF₁, 1:10 000. Antisera against Fd, Cyt *f*, Fox1, Cox2b, and CF₁ were from Agrisera. Antisera against Nuo6–Nuo8 were kindly provided by Patrice Hamel, and antisera against D1, PsaD, and LhcSR were kindly provided by Susan Preiss, Jean-David Rochaix, and Michel Guertin, respectively.

Oxygen evolution

Oxygen evolution rates were measured using a standard Clark-type electrode (Hansatech Oxygraph with a DW-1 chamber). Photosynthetic rate in situ was calculated as: oxygen evolution at $217 \mu\text{mol photons m}^{-2} \text{s}^{-1}$ minus oxygen consumption in the dark. For all other oxygen evolution measurements, cells were collected by centrifugation as described above, resuspended in medium and dark acclimated at 25°C for 10 min. Chlorophyll *a* per sample ranged from 10 to 20 nmol/ml. Cells were placed in the cuvette and nitrogen gas was used to purge dissolved oxygen to about 50% saturation. The respiration rate was measured as oxygen consumption for 5 min in the dark. Changes in oxygen concentration were measured for 30 s at: 3, 8, 21, 46, 71, 84, 88, 218, 358, 544, 650, 927, 1350, and $1735 \mu\text{mol photons m}^{-2} \text{s}^{-1}$ sequentially. 500 μ l of cells was removed from the cuvette at the end of the light

sequence, centrifuged at $14,000 \times g$ for 5 min, and the pellets were resuspended and extracted in 80% acetone for several hours. Chlorophyll *a* concentrations were estimated as described previously (Porra et al. 1989; Porra 2002). These data were used to assemble photosynthesis–irradiance curves. Net oxygen evolution rates were normalized to chlorophyll *a*, and photosynthetic parameters were derived by fitting light saturation curves to the equation: $P = P_{\text{max}} \tanh(\alpha I / P_{\text{max}})$ using Matlab, where *P* is the oxygen evolution rate at a given light intensity (*I*) (Neale and Melis 1986).

Pigment determination

Cells (1 ml) were collected by centrifugation at $14,000 \times g$ in a table-top centrifuge. The medium was removed by aspiration and the pellet was immediately frozen in liquid nitrogen and held at -80°C . The abundance of chlorophyll *a* and xanthophyll cycle pigments was determined by HPLC after extraction in 100% acetone according to Müller-Moulé et al. (2002).

Chlorophyll *a* fluorescence

Chlorophyll *a* fluorescence was measured using a Hansatech FMS2 pulse-modulated fluorometer. Cells were dark acclimated for 15 min and gently filtered onto 13-mm diameter Millipore AP20 glass fiber filters. These filters were placed into the manufacturer's leaf clip and an actinic light intensity of $217 \mu\text{mol photons m}^{-2} \text{s}^{-1}$ was used to probe the photo-physiology of the algal cells. Chlorophyll *a* fluorescence parameters were assayed and calculated according to the definitions of Baker (2008).

Results

Growth of photoheterotrophic versus phototrophic Chlamydomonas

To determine the impact of photoheterotrophic versus phototrophic conditions on the growth of Chlamydomonas, wild-type cells were grown in various concentrations of iron with either acetate or CO₂ supplied as a carbon source. Within carbon source treatments, iron-replete ($20\text{-}\mu\text{M Fe}$) and iron-deficient ($1\text{-}\mu\text{M Fe}$) cultures grew at the same rate, while iron-limited ($\leq 0.2\text{-}\mu\text{M Fe}$) cultures grew at a slower rate. The difference in growth rate as a function of iron nutrition was more pronounced in photoheterotrophic conditions where the growth rate in iron limitation was about half (57%) of the rate in the replete situation when compared to phototrophic conditions where the rate in iron limitation was 75% of that in the replete situation

(Table 1). In the presence of acetate, iron-replete and -deficient cultures reached a final density of 1.5×10^7 cells/ml after 6 days of growth, while iron-limited cultures reached stationary phase in 8 days, achieving a final density of only $5\text{--}9 \times 10^6$ cells/ml (Fig. 1). In contrast, phototrophic iron-replete and -deficient phototrophic cultures reached a density of only 9×10^6 cells/ml, comparable to the final cell density of iron-limited photoheterotrophic cultures (Fig. 1).

Phototrophic cells accumulate more Fe than photoheterotrophic cells

In order to relate the growth rate to iron nutrition, the iron content of cells in the presence and in the absence of acetate was determined by inductively coupled plasma-mass spectroscopy. Surprisingly, when the cells were grown phototrophically, they accumulated approximately twice the amount of iron when compared to photoheterotrophically grown cells in both iron-deficient and -limited conditions (Fig. 2). This cannot be attributed to a difference in iron bioavailability, since acetate does not impact Fe speciation significantly, nor can it be attributed to a larger cell size, since phototrophically grown cells were actually 10–20% smaller in diameter than photoheterotrophically grown cells (data not shown).

Photosynthetic and respiratory capacity of photoheterotrophic versus phototrophic cells

Because photosynthesis and respiration are the two most iron-rich processes in the cell, photosynthetic and respiratory rates were measured to assess the impact of Fe nutrition on these bioenergetic pathways. Our estimates of in situ photosynthetic rates showed that the oxygen evolution rates of photoheterotrophically grown cells (+acetate) decreased as a function of iron nutrition (Table 2). In phototrophic conditions (–acetate), oxygen evolution rates remained comparable to those in iron-replete acetate-grown cells (approximately $6 \text{ nmol ml}^{-1} \text{ min}^{-1}$ per million cells), even under severe iron limitation. Similarly, chlorophyll *a* levels remained steady over a range of iron

concentrations in phototrophically grown cells (approximately $5 \text{ fmol chl } a/\text{cell}$), whereas in the presence of acetate, chlorophyll *a* levels correlated with the amount of iron provided in the medium (Fig. 3). The amount of chlorophyll *a* accumulated in phototrophically grown cells was equivalent to the chlorophyll *a* level of iron-deficient acetate-grown cells ($1\text{-}\mu\text{M Fe}$). Respiration rates were unaffected by iron nutrition, but were affected instead by carbon source. Acetate-grown cells had the ability to respire at a rate approximately two times greater than CO_2 -grown cells ($2 \text{ nmol ml}^{-1} \text{ min}^{-1}$ per million cells vs. $0.7 \text{ nmol ml}^{-1} \text{ min}^{-1}$ per million cells). This is consistent with the increased abundance of respiratory chain components in acetate-grown cells (Naumann et al. 2007). The mechanism contributing to increased abundance of respiratory components in acetate-grown cells is not known. Whole transcriptome analyses (M. Castruita, unpublished) do not give an indication of a specific increase in the expression of genes encoding respiratory components.

Photosynthetic efficiency of photoheterotrophic versus phototrophic cells

Photosynthesis was further assessed by determination of photosynthesis–irradiance curves. In the presence of acetate, the maximum photosynthetic rate (P_{max}) was decreased with respect to decreased iron nutrition (Table 3). Conversely, P_{max} was increased in phototrophically grown severely iron-limited cells ($0.1\text{-}\mu\text{M Fe}$). On the other hand, the relative quantum efficiency of oxygen evolution (α) was decreased in response to decreased iron concentration in both photoheterotrophically and phototrophically grown cells; although, in phototrophic cells the decrease in α is not seen until severe iron limitation ($0.1\text{-}\mu\text{M Fe}$), concomitant with the increase in P_{max} . The increase in P_{max} of phototrophic cells at $0.1\text{-}\mu\text{M Fe}$ results in an increase in the light saturation index (E_k , defined as P_{max}/α).

Maximum quantum efficiency of PSII in photoheterotrophic versus phototrophic cells

F_v/F_m is relatively constant, but decreased in stressed cells (Björkman and Demmig 1987), such as those under iron limitation (Morales et al. 1990, 2000). This parameter, which assesses the maximum quantum efficiency of PSII photochemistry, was lower in iron-limited relative to iron-replete *Chlamydomonas* cells in the presence of acetate, but remained high in iron-limited cells growing phototrophically, indicating maintenance of light reactions and photochemistry (Table 4). Non-photochemical quenching (NPQ) was likewise decreased in iron-limited acetate-grown cells, but remained high (and perhaps slightly

Table 1 Growth rate of photoheterotrophic versus phototrophic cells in response to iron nutrition

Fe (μM)	Acetate μ (day^{-1})	CO_2 μ (day^{-1})
0.1	0.96 ± 0.12	0.56 ± 0.04
0.2	0.90 ± 0.04	0.59 ± 0.07
1	1.44 ± 0.15	0.68 ± 0.11
20	1.68 ± 0.08	0.74 ± 0.06

Standard deviation based on biological triplicates

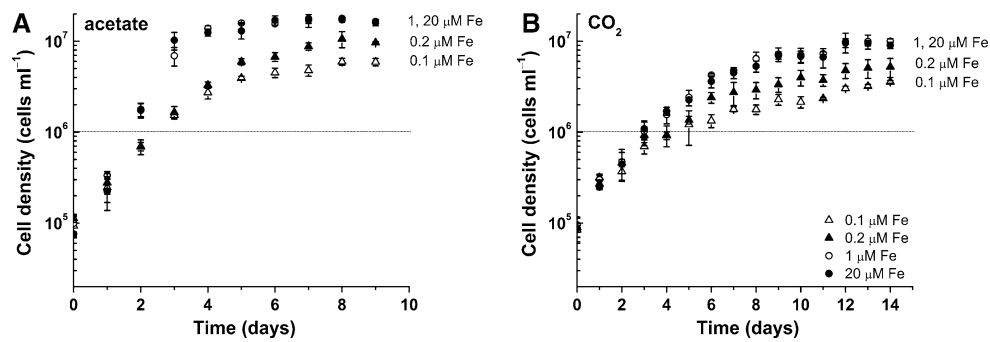


Fig. 1 Growth in photoheterotrophic versus phototrophic growth conditions in response to iron nutrition. Cells were grown in the presence (A) and absence (B) of acetate in various concentrations of iron. Cultures lacking acetate were bubbled with air. Various

concentrations of iron represented by *empty triangles* (0.1- μM Fe), *filled triangles* (0.2- μM Fe), *empty circles* (1- μM Fe), and *filled circles* (20- μM Fe). Standard deviation based on biological triplicates. *Dotted line* indicates cell density at which cells were collected for analysis

Fig. 2 Iron content of photoheterotrophic versus phototrophic cells in various iron concentrations. Cells were grown in the presence (A) and absence (B) of acetate in various concentrations of iron, and iron content was determined by ICP-MS. Error based on three independent experiments. *Asterisk* (*) denotes statistically significant differences between acetate and CO₂ (one-way ANOVA, $P < 0.05$)

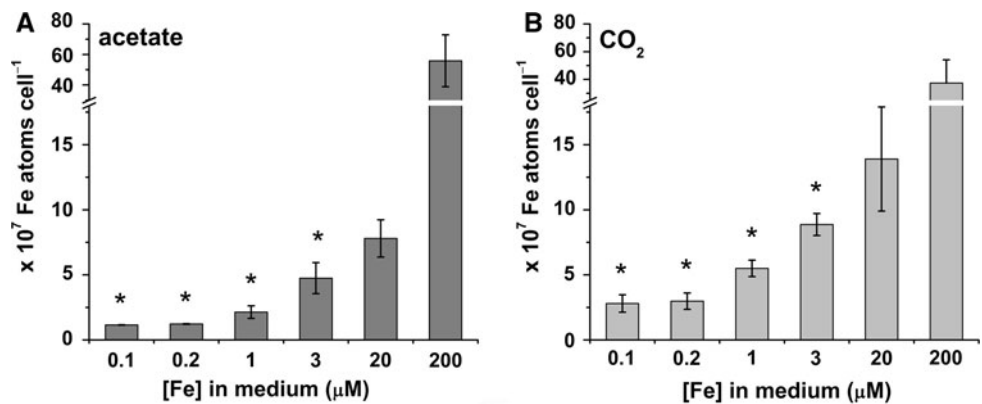


Table 2 Photosynthetic and respiratory rates of acetate versus CO₂-grown cells in various iron concentrations

Fe (μM)	Acetate		CO ₂	
	Photosynthetic rate ^a	Respiration rate ^a	Photosynthetic rate ^a	Respiration rate ^a
0.1	3.1 \pm 0.8	-2.1 \pm 0.4	5.2 \pm 1.4	-0.8 \pm 0.1
0.2	3.4 \pm 0.7	-1.9 \pm 0.2	5.9 \pm 0.8	-0.8 \pm 0.2
1	4.9 \pm 1.2	-1.9 \pm 0.6	6.0 \pm 0.6	-0.6 \pm 0.0
20	6.7 \pm 0.8	-2.5 \pm 0.4	6.1 \pm 0.6	-0.7 \pm 0.1

Photosynthesis measured at 217 $\mu\text{mol photons m}^{-2} \text{s}^{-1}$. Standard deviation based on biological triplicates

^a $\text{nmol ml}^{-1} \text{min}^{-1} 10^6 \text{ cells}^{-1}$

increased) in iron-limited cells without acetate (Fig. 4). This suggests that increased NPQ contributes to the ability of phototrophic iron-limited cells to maintain photosynthesis. At a biochemical level, the abundance of photoprotective xanthophyll cycle pigments was increased in photoheterotrophic iron-limited cells when compared to phototrophic iron-limited cells (Fig. 5). This demonstrates that the up-regulation of photoprotective xanthophyll cycle pigments does not necessarily translate to an increase in NPQ. The redox state of the plastoquinone pool is a result

of a balance between electron transfer in and electron transfer out of the pool. It is estimated by the parameter $(1 - q_L)$. The pool is more reduced in acetate-grown iron-limited cells, which could be attributed to a failure of PSI to draw electrons out of the pool or activation of a mechanism (such as chlororespiration) to increase electron flow into the pool (Fig. 6). The fact that the pool remained reduced in these cells even in the dark suggests the activation of a mechanism for acetate-dependent reduction of the plastoquinone pool in iron-limited cells.

Fig. 3 Chlorophyll *a* content of photoheterotrophic versus phototrophic cells. Cells were grown in the presence (A) and absence (B) of acetate in various concentrations of iron and chlorophyll *a* abundance was determined by HPLC. Standard deviation based on biological triplicates

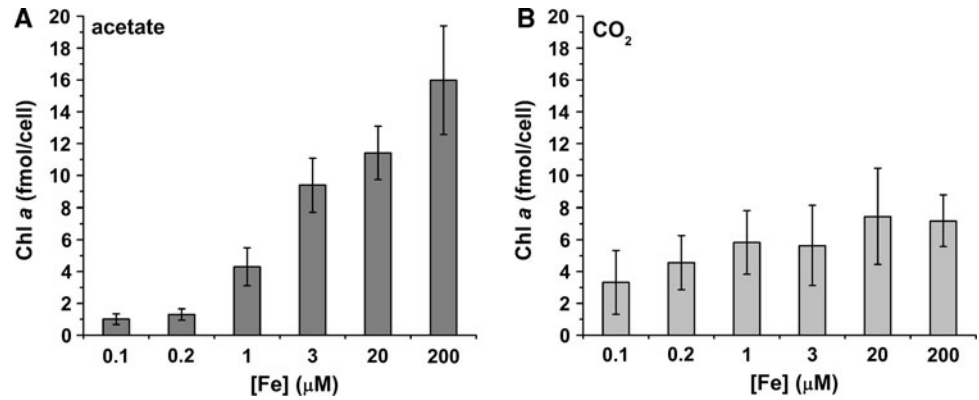


Table 3 Photosynthetic parameters

Fe (μM)	Acetate			CO ₂		
	P_{\max}^a	α^b	$E_k(P_{\max}/\alpha)^c$	P_{\max}^a	α^b	$E_k(P_{\max}/\alpha)^c$
0.1	1.7 ± 0.1	0.014 ± 0.001	130 ± 6	3.6 ± 0.2	0.013 ± 0.004	300 ± 140
0.2	1.9 ± 0.0	0.014 ± 0.002	140 ± 21	2.8 ± 0.2	0.021 ± 0.001	140 ± 16
1	2.3 ± 0.2	0.024 ± 0.002	95 ± 1	2.5 ± 0.2	0.022 ± 0.003	120 ± 11
20	2.7 ± 0.4	0.023 ± 0.002	120 ± 25	2.7 ± 0.2	0.022 ± 0.002	120 ± 7

Standard deviation based on biological triplicates

^a nmol O₂ (nmol Chl *a*)⁻¹ min⁻¹

^b (nmol O₂ [nmol Chl *a*]⁻¹ min⁻¹)/(μmol photons m⁻² s⁻¹)

^c μmol photons m⁻² s⁻¹

Abundance of Fe-containing components in energy transducing membranes

The abundance of photosynthetic and respiratory proteins was determined by immunoblot analysis (Fig. 7). The levels of all photosynthetic Fe-containing proteins investigated were more decreased in response to iron-deficiency in photoheterotrophically grown cells when compared to phototrophically grown cells, which is consistent with our measurements of activity. While the iron-containing

Table 4 Maximum quantum efficiency of PSII in phototrophic versus photoheterotrophic cells in response to iron nutrition

Fe (μM)	F_v/F_m	
	Acetate	CO ₂
0.1	0.54 ± 0.07*	0.72 ± 0.01
0.2	0.67 ± 0.01	0.70 ± 0.02
1	0.73 ± 0.02	0.72 ± 0.01
3	0.73 ± 0.01	0.72 ± 0.01
20	0.74 ± 0.01	0.72 ± 0.01
200	0.74 ± 0.01	0.72 ± 0.00

Standard deviation based on biological triplicates

* Statistically significant difference relative to 20 μM Fe (one-way ANOVA, $P < 0.05$)

photosynthetic proteins ferredoxin (Fd) and cytochrome *f* (Cyt *f*) were already decreased 75% in iron-deficient (1-μM Fe) relative to iron-replete photoheterotrophic cells, phototrophic cells retained their iron-containing proteins until severely iron-limited conditions (0.1-μM Fe). To establish that the decrease in abundance of iron-containing proteins is a specific response to iron deficiency rather than to growth inhibition, we monitored the abundance of Fe-independent proteins LhcSR and ferroxidase (Fox1) whose expression increases in iron-deficient cells (La Fontaine et al. 2002; Naumann et al. 2007). Indeed, the expression of Fox1, a marker of Fe-deficiency, was reciprocal to the abundance of Fe-containing photosynthetic proteins (Fig. 7). The abundance of LhcSR, which is necessary for NPQ (Peers et al. 2009), increased with respect to iron limitation in the photoheterotrophic cells, but was abundant in phototrophic cells, irrespective of Fe-nutritional status. Like ferredoxin and cytochrome *f*, the non-Fe-containing PSII and PSI core proteins, D1 and PsaD, respectively, were also decreased 75% in photoheterotrophic iron-limited cells (0.1 μM Fe) but maintained in phototrophic iron-limited cells (Fig. 7).

Although photosynthesis requires more iron due to the high abundance of photosynthetic complexes in the thylakoid membrane, the demand for iron per monomer is

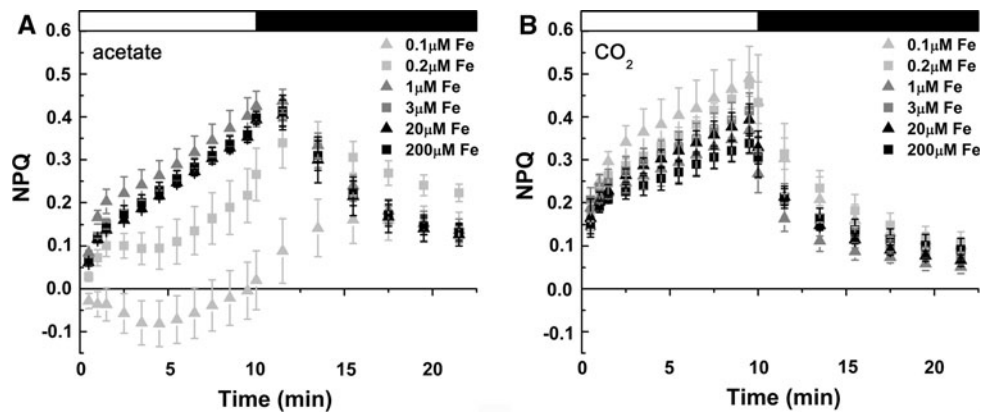


Fig. 4 Non-photochemical quenching of photoheterotrophic versus phototrophic cells in response to iron nutrition. Cells were grown in the presence (A) and absence (B) of acetate in various concentrations of iron. Cells were dark acclimated for 15 min and probed with an actinic light intensity of $217 \mu\text{mol photons m}^{-2} \text{s}^{-1}$. Various

concentrations of iron represented by *gray triangles* (0.1- $\mu\text{M Fe}$), *gray squares* (0.2- $\mu\text{M Fe}$), *dark gray triangles* (1- $\mu\text{M Fe}$), *dark gray squares* (3- $\mu\text{M Fe}$), *black triangles* (20- $\mu\text{M Fe}$), and *black squares* (200- $\mu\text{M Fe}$). Standard deviation based on biological triplicates

Fig. 5 Abundance of the xanthophyll cycle pigments in photoheterotrophic versus phototrophic cells in response to iron nutrition. Cells were grown in the presence (A) and absence (B) of acetate in various concentrations of iron, and the abundance of xanthophyll cycle pigments was determined by HPLC. Average of biological triplicate samples shown

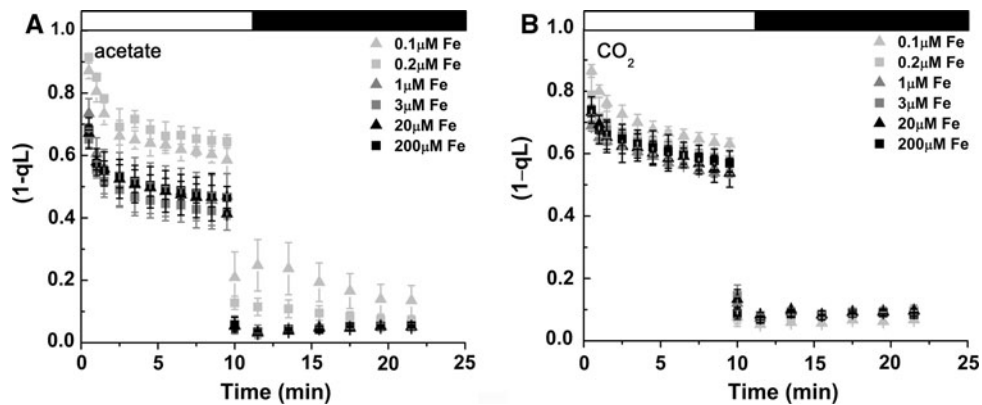
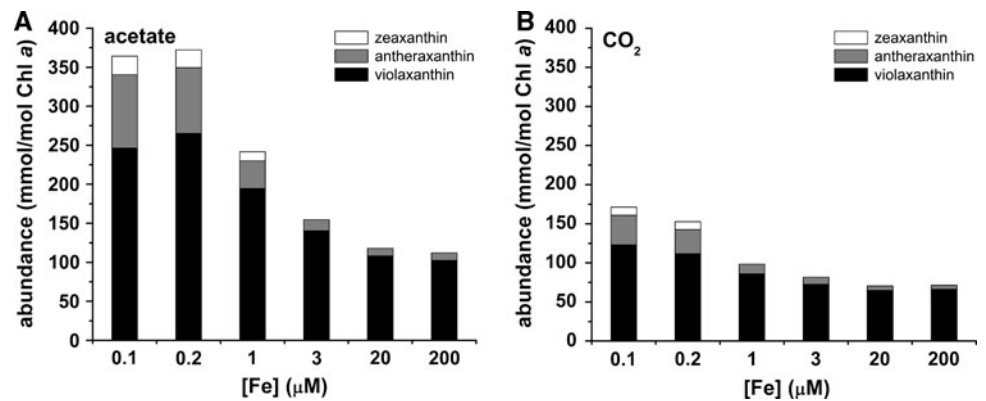


Fig. 6 Estimation of the redox state of the plastoquinone pool of photoheterotrophic versus phototrophic cells in response to iron nutrition. Cells were grown in the presence (A) and absence (B) of acetate in various concentrations of iron. Cells were dark acclimated for 15 min and probed with an actinic light intensity of $217 \mu\text{mol photons m}^{-2} \text{s}^{-1}$. Various

concentrations of iron represented by *gray triangles* (0.1- $\mu\text{M Fe}$), *gray squares* (0.2- $\mu\text{M Fe}$), *dark gray triangles* (1- $\mu\text{M Fe}$), *dark gray squares* (3- $\mu\text{M Fe}$), *black triangles* (20- $\mu\text{M Fe}$), and *black squares* (200- $\mu\text{M Fe}$). Standard deviation based on biological triplicates

greater for respiration. Complex I requires the most iron, containing a total of 8 iron–sulfur clusters (6 $[\text{Fe}_4\text{S}_4]$ and 2 $[\text{Fe}_2\text{S}_2]$) for a total of 28 Fe atoms per complex I (Cardol

et al. 2004; Sazanov 2007; Remacle et al. 2008). Complex II binds a total of 9 Fe atoms in the form of 3 iron–sulfur clusters (1 $[\text{Fe}_2\text{S}_2]$, 1 $[\text{Fe}_3\text{S}_4]$, and 1 $[\text{Fe}_4\text{S}_4]$) and 1 heme.

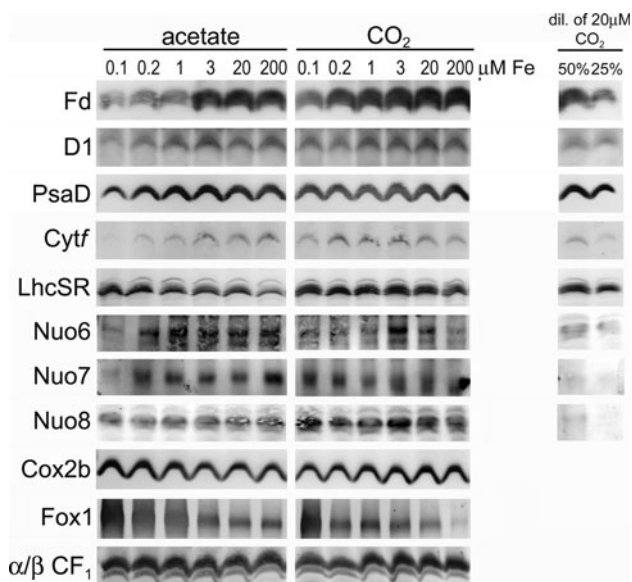


Fig. 7 Abundance of photosynthetic and respiratory proteins in photoheterotrophic versus phototrophic cells in response to iron nutrition. 20 μg of total protein was separated by denaturing polyacrylamide gel electrophoresis and immunoblotted for various photosynthetic and respiratory proteins. One of three representative experiments is shown

Complex III contains 5 Fe atoms bound to 1 $[\text{Fe}_2\text{S}_2]$ and 3 heme molecules, and complex IV utilizes 2 heme molecules to reduce oxygen to water. Since complex I contains the most iron, the abundance of iron-binding subunits of complex I was investigated. Surprisingly, similar to photosynthetic proteins, complex I subunits Nuo6 (Fe/S-binding) and Nuo7 (non-Fe/S-binding) were maintained in iron-limited (0.1- μM Fe) phototrophic cells, but decreased approximately 2-fold in heterotrophic iron-limited cells, even though iron-limited heterotrophic cells had a higher rate of oxygen consumption (Fig. 7; Table 2). Fe/S-binding Nuo8 was also more abundant in phototrophic when compared to photoheterotrophic cells (Fig. 7).

Since oxygen consumption rates measured in Table 2 are a direct result of complex IV activity, complex IV (Cox2b) abundance was investigated. Like complex I proteins, Cox2b was also maintained in phototrophic cells, and was slightly increased in iron-limited photoheterotrophic cells (Fig. 7), in agreement with the insensitivity of respiratory rate to iron limitation in the presence of acetate (Table 2). Collectively, these results indicate that phototrophic cells accumulate more iron, and are therefore able to maintain both photosynthetic and respiratory electron transport chain proteins, and this correlates with their increased capacity for iron accumulation, resulting probably from increased expression of iron uptake components.

Discussion

Respiration is preferred over photosynthesis in iron-limited *Chlamydomonas*

In this study, we investigated the impact of iron limitation on photosynthesis and respiration of *Chlamydomonas* in the presence and in the absence of acetate. Overall, the results indicated that respiration is the preferred bioenergetic pathway in *Chlamydomonas* cells when a substrate is available. Photoheterotrophic cells, given the option to grow phototrophically or heterotrophically, suppressed photosynthetic iron-containing proteins before iron-containing respiratory proteins in response to decreasing iron nutrition (Fig. 7). In the presence of acetate, iron-limited cells could respire at a rate approximately three times that of iron-replete phototrophic cells (Table 2). In addition, the growth rate of severely iron-limited photoheterotrophic cells was still faster than the growth rate of iron-replete photoautotrophic cells (Table 1; Fig. 1). These results are consistent with theoretical predictions of iron use efficiencies (carbon fixed into cellular biomass per unit Fe per unit time), which suggest that cells growing via respiration alone are more efficient than those employing photosynthesis (Raven 1988). Collectively, these data indicate that when given a choice, it is more effective for the organism to use respiration instead of photosynthesis.

In a study of the response of photoheterotrophic *Chlamydomonas* to iron-starvation using a proteomics approach, photosynthetic proteins were decreased while respiratory proteins were increased, suggesting the prioritization of respiration over photosynthesis in iron deficiency (Naumann et al. 2007). In that study, a 20% decrease in the abundance of respiratory complex I subunits was observed in iron-starved cells, while all other respiratory components were increased in abundance. This may be due to the fact that the Fe in Fe/S is more labile than Fe bound to heme (Fridovich 1997; Imlay 2006; Jang and Imlay 2007). In agreement with these results, the decrease of complex I subunits in iron-limited photoheterotrophic cells and an increase in Cox2b were also observed in this study (Fig. 7).

Phototrophic cells are less sensitive to iron deficiency

In general, phototrophic cells are less sensitive to iron-deficiency than are photoheterotrophic cells. This could be observed at the level of growth rate, where the difference in growth rate of iron-replete versus iron-limited cells was much more drastic in photoheterotrophic (57%) than in phototrophic (75%) conditions (Table 1; Fig. 1). Iron-limited phototrophic cells were also visually less impacted with respect to chlorosis than photoheterotrophic cells

(data not shown), and this was confirmed by HPLC analysis of chlorophyll *a* levels (Fig. 3). A similar trend was observed for oxygen evolution rates. While oxygen evolution rates were decreased at least 50% in response to iron limitation in acetate-grown cells, they were only decreased 10% in phototrophic iron-limited cells relative to iron-replete conditions (Table 2). The lack of sensitivity is also noted with respect to respiration and the maintenance of respiratory and photosynthetic complexes (Fig. 7). We attribute this to the higher iron content (and hence reservoir) in phototrophic versus photoheterotrophic cells (Fig. 2). It is possible that the excess iron is stored in ferritin or the vacuole of phototrophic cells and provided as needed as cells divide and deplete iron from the medium (Long et al. 2008; Roschztardt et al. 2009). Although the lower abundance of ferritin as measured by immunoblot analysis in phototrophic cells (Supplemental Fig. 1; Busch et al. 2008) might argue against this possibility, we note that in neither study was the iron content of ferritin assessed. Since the mechanisms for regulating iron loading and unloading of ferritin are not known, storage in ferritin remains a formal possibility. Another possibility is that more iron may be stored in the vacuole of phototrophic cells relative to photoheterotrophic cells and mobilized in a situation of iron-deficiency by up-regulation of vacuolar efflux transporters. Both the vacuole and the ferritin have been implicated as possible sites of iron storage in *Chlamydomonas* as well as in other plants (Semin et al. 2003; Lanquar et al. 2005; Kim et al. 2006; Long et al. 2008; Briat et al. 2009). According to ferroxidase expression, which we use as a sentinel of iron nutritional status, phototrophic cells are not iron-deficient until the iron in the medium is lowered to 0.1 μM (Fig. 7), which supports the model of iron storage in phototrophic cells. The delayed degradation of PSI and expression of ferroxidase in phototrophic cells was also observed in an iron starvation time course experiment of cells grown in TAP versus HSM medium (Busch et al. 2008).

It is interesting to note that the abundance of de-epoxidized xanthophyll cycle pigments was increased in photoheterotrophic iron-limited cells when compared to phototrophic iron-limited cells (Fig. 5), and LhcSR proteins were expressed at similar levels (Fig. 7), yet iron-limited photoheterotrophic cells were clearly impaired in NPQ (Fig. 4). This result suggests that the presence of de-epoxidized xanthophyll pigments and LhcSR proteins is not sufficient for NPQ, and that another factor is necessary to induce NPQ. Although photoheterotrophic iron-limited cells can generate a thylakoid lumen pH low enough to induce the xanthophyll cycle, it is possible that the decreased capacity for photosynthetic electron transport in these cells is unable to maintain a lumen pH that is low enough to induce NPQ to the same extent as in

phototrophic cells. This result could also indicate that LhcSR proteins are required for functions other than NPQ.

We noted that the plastoquinone pool of iron-limited photoheterotrophic cells was more reduced, even in the dark (Fig. 6). The reduction of plastoquinone is known to occur in *Chlamydomonas* by chlororespiration via a nucleus-encoded type-II NAD(P)H dehydrogenase (Mus et al. 2005; Jans et al. 2008; Desplats et al. 2009). In the light, one possibility is that the observed reduction of the plastoquinone pool in iron-limited photoheterotrophic cells is due in part to a reduced number of PSI centers in iron-limited cells (Moseley et al. 2002).

In conclusion, in the presence of acetate, iron-limited *Chlamydomonas* cells maintain high growth rates by suppressing photosynthesis and prioritizing respiration, while phototrophic cells maintain efficient photosynthetic systems throughout the spectrum of iron status, but still lose overall photosynthetic capacity at the onset of iron deficiency, which is delayed in phototrophic cells (0.1- μM Fe vs. 1- μM Fe in photoheterotrophic cells) due to their increased iron content.

Acknowledgments We thank Patrice Hamel for antibodies against Nuo6-8, Susanne Preiss for antibodies against D1, Michel Guertin for antibodies against LhcSR, and Jean-David Rochoaix for antibodies against Psad. We are grateful to Janette Kropat for the measurement of iron shown in Fig. 2 and to Marina Sharifi for assistance with HPLC analysis, to Davin Malasarn for his assistance with Visual Minteq and to Naomi Ginsberg for extrapolating the data shown in Table 3 using Matlab. This research was supported by grants from the Department of Energy (DE-FD02-04ER15529) to S.S.M. and from the Chemical Sciences, Geosciences and Biosciences Division, Office of Basic Energy Sciences, Office of Science, U.S. Department of Energy (FWP number 449A449B) to K.K.N. Aimee Terauchi was supported by an Institutional Ruth L. Kirschstein National Research Service Award (GM070104) and a Dissertation Year Fellowship from the UCLA graduate division.

Open Access This article is distributed under the terms of the Creative Commons Attribution Noncommercial License which permits any noncommercial use, distribution, and reproduction in any medium, provided the original author(s) and source are credited.

References

- Andaluz S, López-Millán A-F, De las Rivas J, Aro E-M, Abadía J, Abadía A (2006) Proteomic profiles of thylakoid membranes and changes in response to iron deficiency. *Photosynth Res* 89:141–155
- Baker NR (2008) Chlorophyll fluorescence: a probe of photosynthesis in vivo. *Annu Rev Plant Biol* 59:89–113
- Björkman O, Demmig B (1987) Photon yield of O₂ evolution and chlorophyll fluorescence characteristics at 77 K among vascular plants of diverse origins. *Planta* 170:489–504
- Boyd PW, Watson AJ, Law CS, Abraham ER, Trull T, Murdoch R, Bakker DCE, Bowie AR, Buesseler KO, Chang H et al (2000) A mesoscale phytoplankton bloom in the polar Southern Ocean stimulated by iron fertilization. *Nature* 407:695–702

- Briat JF, Curie C, Gaymard F (2007) Iron utilization and metabolism in plants. *Curr Opin Plant Biol* 10:276–282
- Briat JF, Duc C, Ravet K, Gaymard F (2009) Ferritins and iron storage in plants. *Biochim Biophys Acta*. doi: [10.1016/j.bbagen.2009.10.12.1003](https://doi.org/10.1016/j.bbagen.2009.10.12.1003)
- Busch A, Rimbauld B, Naumann B, Rensch S, Hippler M (2008) Ferritin is required for rapid remodeling of the photosynthetic apparatus and minimizes photo-oxidative stress in response to iron availability in *Chlamydomonas reinhardtii*. *Plant J* 55:201–211
- Cardol P, Vanrobaeys F, Devreese B, Van Beeumen J, Matagne RF, Remacle C (2004) Higher plant-like subunit composition of mitochondrial complex I from *Chlamydomonas reinhardtii*: 31 conserved components among eukaryotes. *Biochim Biophys Acta* 1658:212–224
- Desplats C, Mus F, Cuiné S, Billon E, Cournac L, Peltier G (2009) Characterization of Nda2, a plastoquinone-reducing Type II NAD(P)H dehydrogenase in *Chlamydomonas* chloroplasts. *J Biol Chem* 284:4148–4157
- Erdner DL, Price NM, Doucette GJ, Peleato ML, Anderson DM (1999) Characterization of ferredoxin and flavodoxin as markers of iron limitation in marine phytoplankton. *Mar Ecol Prog Ser* 184:43–53
- Fridovich I (1997) Superoxide anion radical ($O_2^{\cdot-}$), superoxide dismutases, and related matters. *J Biol Chem* 272:18515–18517
- Greene RM, Geider RJ, Kolber Z, Falkowski PG (1992) Iron-induced changes in light harvesting and photochemical energy conversion processes in eukaryotic marine algae. *Plant Physiol* 100:565–575
- Guerinot ML (1994) Microbial iron transport. *Annu Rev Microbiol* 48:743–772
- Guerinot ML, Yi Y (1994) Iron: nutritious, noxious, and not readily available. *Plant Physiol* 104:815–820
- Harris EH (2009) The *Chlamydomonas* sourcebook: introduction to *Chlamydomonas* and its laboratory use, vol 1, 2nd edn. Academic Press, San Diego
- Howe G, Merchant S (1992) The biosynthesis of membrane and soluble plastidic c-type cytochromes of *Chlamydomonas reinhardtii* is dependent on multiple common gene products. *EMBO J* 11:2789–2801
- Hubbard JAM, Lewandowska KB, Hughes MN, Poole RK (1986) Effects of iron limitation of *Escherichia coli* on growth, the respiratory chains and gallium uptake. *Arch Microbiol* 146:80–86
- Imlay JA (2006) Iron-sulphur clusters and the problem with oxygen. *Mol Microbiol* 59:1073–1082
- Ivanov AG, Park YI, Miskiewicz E, Raven JA, Huner NPA, Öquist G (2000) Iron stress restricts photosynthetic intersystem electron transport in *Synechococcus* sp. PCC 7942. *FEBS Lett* 485:173–177
- Jang S, Imlay JA (2007) Micromolar intracellular hydrogen peroxide disrupts metabolism by damaging iron-sulfur enzymes. *J Biol Chem* 282:929–937
- Jans F, Mignolet E, Houyoux PA, Cardol P, Ghysels B, Cuiné S, Cournac L, Peltier G, Remacle C, Franck F (2008) A type II NAD(P)H dehydrogenase mediates light-independent plastoquinone reduction in the chloroplast of *Chlamydomonas*. *Proc Natl Acad Sci USA* 105:20546–20551
- Kim SA, Punshon T, Lanzirrotti A, Li L, Alonso JM, Ecker JR, Kaplan J, Guerinot ML (2006) Localization of iron in Arabidopsis seed requires the vacuolar membrane transporter VIT1. *Science* 314:1295–1298
- Kouril R, Arteni AA, Lax J, Yeremenko N, D’Haene S, Rögner M, Matthijs HCP, Dekker JP, Boekema EJ (2005) Structure and functional role of supercomplexes of IsiA and photosystem I in cyanobacterial photosynthesis. *FEBS Lett* 579:3253–3257
- La Fontaine S, Quinn JM, Nakamoto SS, Page MD, Gohre V, Moseley JL, Kropat J, Merchant S (2002) Copper-dependent iron assimilation pathway in the model photosynthetic eukaryote *Chlamydomonas reinhardtii*. *Eukaryot Cell* 1:736–757
- La Roche J, Murray H, Orellana M, Newton J (1995) Flavodoxin expression as an indicator of iron limitation in marine diatoms. *J Phycol* 31:520–530
- La Roche J, Boyd PW, McKay RML, Geider RJ (1996) Flavodoxin as an in situ marker for iron stress in phytoplankton. *Nature* 382:802–805
- Lanquar V, Lelièvre F, Bolte S, Hamès C, Alcon C, Neumann D, Vansuyt G, Curie C, Schröder A, Krämer U et al (2005) Mobilization of vacuolar iron by AtNRAMP3 and AtNRAMP4 is essential for seed germination on low iron. *EMBO J* 24:4041–4051
- Laudenbach DE, Reith ME, Straus NA (1988) Isolation, sequence analysis, and transcriptional studies of the flavodoxin gene from *Anacystis nidulans* R2. *J Bacteriol* 170:258–265
- Long JC, Merchant SS (2008) Photo-oxidative stress impacts the expression of genes encoding iron metabolism components in *Chlamydomonas*. *Photochem Photobiol* 84:1395–1403
- Long JC, Sommer F, Allen MD, Lu SF, Merchant SS (2008) *FER1* and *FER2* encoding two ferritin complexes in *Chlamydomonas reinhardtii* chloroplasts are regulated by iron. *Genetics* 179:137–147
- López-Millán AF, Morales F, Andaluz S, Gogorcena Y, Abadía A, Rivas JDL, Abadía J (2000) Responses of sugar beet roots to iron deficiency. Changes in carbon assimilation and oxygen use. *Plant Physiol* 124:885–898
- Marschner H, Römheld V (1994) Strategies of plants for acquisition of iron. *Plant Soil* 165:261–274
- Martin JH, Coale KH, Johnson KS, Fitzwater SE, Gordon RM, Tanner SJ, Hunter CN, Elrod VA, Nowicki JL, Coley TL et al (1994) Testing the iron hypothesis in ecosystems of the equatorial Pacific Ocean. *Nature* 371:123–129
- Michel KP, Pistorius EK (2004) Adaptation of the photosynthetic electron transport chain in cyanobacteria to iron deficiency: the function of IdiA and IsiA. *Physiol Plant* 120:36–50
- Morales F, Abadía A, Abadía J (1990) Characterization of the xanthophyll cycle and other photosynthetic pigment changes induced by iron deficiency in Sugar Beet (*Beta vulgaris* L.). *Plant Physiol* 94:607–613
- Morales F, Belkhdja R, Abadía A, Abadía J (2000) Photosystem II efficiency and mechanisms of energy dissipation in iron-deficient, field-grown pear trees (*Pyrus communis* L.). *Photosynth Res* 63:9–21
- Moseley JL, Allinger T, Herzog S, Hoerth P, Wehinger E, Merchant S, Hippler M (2002) Adaptation to Fe-deficiency requires remodeling of the photosynthetic apparatus. *EMBO J* 21:6709–6720
- Müller-Moulé P, Conklin PL, Niyogi KK (2002) Ascorbate deficiency can limit violaxanthin de-epoxidase activity in vivo. *Plant Physiol* 128:970–977
- Mus F, Cournac L, Cardellini V, Caruana A, Peltier G (2005) Inhibitor studies on non-photochemical plastoquinone reduction and H₂ photoproduction in *Chlamydomonas reinhardtii*. *Biochim Biophys Acta* 1708:322–332
- Naumann B, Stauber EJ, Busch A, Sommer F, Hippler M (2005) N-terminal processing of Lhca3 is a key step in remodeling of the photosystem I-light-harvesting complex under iron deficiency in *Chlamydomonas reinhardtii*. *J Biol Chem* 280:20431–20441
- Naumann B, Busch A, Allmer J, Ostendorf E, Zeller M, Kirchhoff H, Hippler M (2007) Comparative quantitative proteomics to investigate the remodeling of bioenergetic pathways under iron deficiency in *Chlamydomonas reinhardtii*. *Proteomics* 7:3964–3979
- Neale PJ, Melis A (1986) Algal photosynthetic membrane complexes and the photosynthesis-irradiance curve: a comparison of light-

- adaptation responses in *Chlamydomonas reinhardtii* (Chlorophyta). *J Phycol* 22:531–538
- Pascal N, Douce R (1993) Effect of iron deficiency on the respiration of Sycamore (*Acer pseudoplatanus* L.) cells. *Plant Physiol* 103:1329–1338
- Peers G, Truong TB, Ostendorf E, Busch A, Elrad D, Grossman AR, Hippler M, Niyogi KK (2009) An ancient light-harvesting protein is critical for the regulation of algal photosynthesis. *Nature* 462:518–521
- Petroutsos D, Terauchi AM, Busch A, Hirschmann I, Merchant SS, Finazzi G, Hippler M (2009) PGRL1 participates in iron-induced remodeling of the photosynthetic apparatus and in energy metabolism in *Chlamydomonas reinhardtii*. *J Biol Chem* 284:32770–32781
- Philpott CC (2006) Iron uptake in fungi: a system for every source. *Biochim Biophys Acta* 1763:636–645
- Porra RJ (2002) The chequered history of the development and use of simultaneous equations for the accurate determination of chlorophylls *a* and *b*. *Photosynth Res* 73:149–156
- Porra RJ, Thompson WA, Kriedemann PE (1989) Determination of accurate extinction coefficients and simultaneous equations for assaying chlorophylls *a* and *b* extracted with four different solvents: verification of the concentration of chlorophyll standards by atomic absorption spectroscopy. *Biochim Biophys Acta* 975:384
- Rainnie DJ, Bragg PD (1973) The effect of iron deficiency on respiration and energy-coupling in *Escherichia coli*. *J Gen Microbiol* 77:339–349
- Raven JA (1988) The iron and molybdenum use efficiencies of plant growth with different energy, carbon and nitrogen sources. *New Phytol* 109:279–287
- Remacle C, Barbieri M, Cardol P, Hamel PP (2008) Eukaryotic complex I: functional diversity and experimental systems to unravel the assembly process. *Mol Genet Genomics* 280:93–110
- Roschttardt H, Conejero G, Curie C, Mari S (2009) Identification of the endodermal vacuole as the iron storage compartment in the *Arabidopsis* embryo. *Plant Physiol* 151:1329–1338
- Sandmann G, Malkin R (1983) Iron-sulfur centers and activities of the photosynthetic electron transport chain in iron-deficient cultures of the blue-green alga *Aphanocapsa*. *Plant Physiol* 73:724–728
- Sandmann G, Peleato ML, Fillat MF, Lázaro MC, Gómez-Moreno C (1990) Consequences of the iron-dependent formation of ferredoxin and flavodoxin on photosynthesis and nitrogen fixation on *Anabaena* strains. *Photosynth Res* 26:119–125
- Sazanov LA (2007) Respiratory complex I: mechanistic and structural insights provided by the crystal structure of the hydrophilic domain. *Biochemistry* 46:2275–2288
- Semin BK, Davletshina LN, Novakova AA, Kiseleva TyY, Lanchinskaya VY, Aleksandrov AY, Seifulina N, Ivanov IyI, Seibert M, Rubin AB (2003) Accumulation of ferrous iron in *Chlamydomonas reinhardtii*. Influence of CO₂ and anaerobic induction of the reversible hydrogenase. *Plant Physiol* 131:1756–1764
- Singh AK, McIntyre LM, Sherman LA (2003) Microarray analysis of the genome-wide response to iron deficiency and iron reconstitution in the cyanobacterium *Synechocystis* sp. PCC 6803. *Plant Physiol* 132:1825–1839
- Straus NA (1995) Iron deprivation: physiology and gene regulation. In: *The molecular biology of cyanobacteria*. Kluwer Academic Publisher, Dordrecht, pp. 731–750
- Strzepek RF, Harrison PJ (2004) Photosynthetic architecture differs in coastal and oceanic diatoms. *Nature* 431:689–692
- Terauchi AM, Lu SF, Zaffagnini M, Tappa S, Hirasawa M, Tripathy JN, Knaff DB, Farmer PJ, Lemaire SD, Hase T, Merchant SS (2009) Pattern of expression and substrate specificity of chloroplast ferredoxins from *Chlamydomonas reinhardtii*. *J Biol Chem* 284:25867–25878
- Tortell PD, Maldonado MT, Price NM (1996) The role of heterotrophic bacteria in iron-limited ocean ecosystems. *Nature* 383:330–332
- Tottey S, Block MA, Allen M, Westergren T, Albrieux C, Scheller HV, Merchant S, Jensen PE (2003) *Arabidopsis* CHL27, located in both envelope and thylakoid membranes, is required for the synthesis of protochlorophyllide. *Proc Natl Acad Sci USA* 100:16119–16124
- Vassiliev IR, Kolber Z, Wyman KD, Mauzerall D, Shukla VK, Falkowski PG (1995) Effects of iron limitation on photosystem II composition and light utilization in *Dunaliella tertiolecta*. *Plant Physiol* 109:963–972
- Vigani G, Maffi D, Zocchi G (2009) Iron availability affects the function of mitochondria in cucumber roots. *New Phytol* 182:127–136
- Walker EL, Connolly EL (2008) Time to pump iron: iron-deficiency-signaling mechanisms of higher plants. *Curr Opin Plant Biol* 11:530–535